

[Electronic Supplementary Information (ESI)]

Comparative Study of Photoinduced Surface-relief-gratings on Azo Polymer and Azo Molecular Glass Films

Xu Li, Hao Huang, Bing Wu, Chuyi Liao and Xiaogong Wang*

*Department of Chemical Engineering, Laboratory of Advanced Materials (MOE),
Tsinghua University, Beijing 100084, P. R. China*

* Corresponding author. E-mail address: wxg-dce@mail.tsinghua.edu.cn

1. Synthesis of BP-AZ-CA and IAC-4

Synthesis of BP-AN. BP-AN was used as a precursor polymer to prepare BP-AZ-CA through post polymerization azo-coupling reaction scheme, which was synthesized according to literature.^{S1} Diglycidyl ether of bisphenol-A (7.60 g, 20 mmol) and aniline (1.86 g, 20 mmol) were mixed under a slow heating condition. After melted and well mixed, the mixture was kept at 110 °C for 72 h. The solid obtained from the reaction was dissolved in 100 mL mixed solvent of chloroform/methanol (vol/vol = 4/1) and precipitated with plenty of petroleum ether. BP-AN as white solid was obtained after vacuum drying at 70 °C for 24 h.

Synthesis of BP-AZ-CA. BP-AN (4.33 g, 10 mmol) was dissolved in DMF (330 mL) at 0 °C. A diazonium salt of *p*-aminobenzoic acid was prepared by adding an aqueous solution of sodium nitrite (1.0 g, 14.4 mmol in 3 mL of water) into a solution of *p*-aminobenzoic acid (1.65 g, 12 mmol) and sodium hydroxide (0.48 g, 12 mmol) in a homogeneous mixture of 3 mL of hydrochloric acid and 15 mL of deionized water. The mixture was stirred at 0 °C for 5 min and then was added dropwise into the BP-AN solution. The solution was stirred at 0 °C for 12 h and then slowly poured into plenty of water, and the precipitate was collected by filtration and dried at 70 °C for 24 h. The product was dissolved in 100 mL THF again and precipitated into 500 mL petroleum ether. A red solid as the final product was obtained after vacuum drying at 70 °C for 24 h.

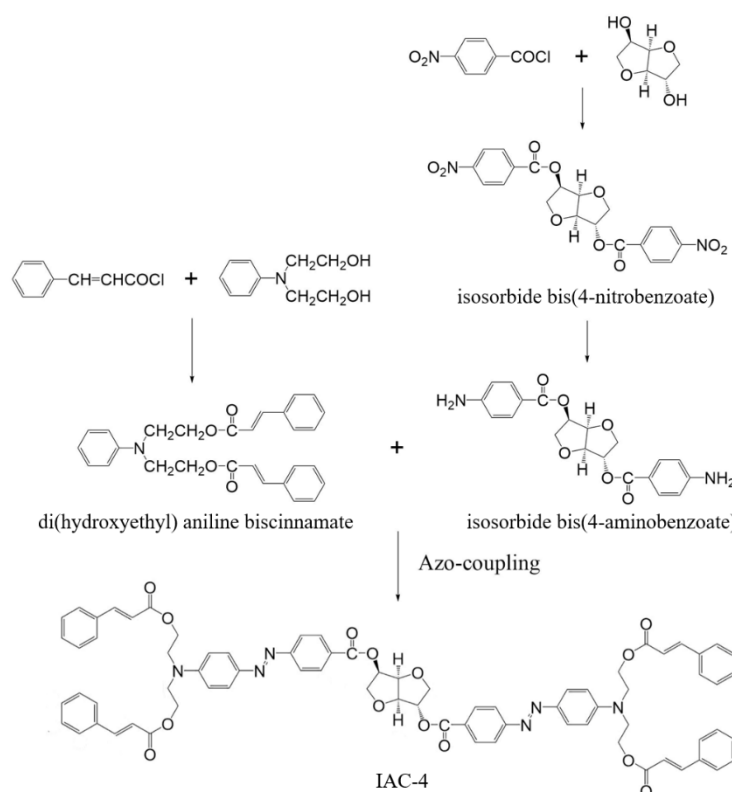
The azo molecular glass IAC-4 was synthesized through the route shown in Scheme S1 according to our previous paper,^{S2} which is described below in detail.

Synthesis of isosorbide bis(4-nitrobenzoate). Isosorbide (7.31 g, 0.05 mol) and triethylamine (15 mL) were dissolved in DMF (50 mL), and the mixture was stirred in an ice-water bath. 4-Nitrobenzoyl chloride was dissolved in DMF (100 mL) and added dropwise into the mixture. The reaction was carried out at room temperature for 6 h. After the reaction, the mixture was washed with saturated salt water and dried. White solid was obtained after washing with hot alcohol and distillation under vacuum.

Synthesis of isosorbide bis(4-aminobenzoate). Isosorbide bis(4-nitrobenzoate) (18.8 g, 0.042 mol), sodium sulfide nonahydrate (57.6 g, 0.24 mol) and ammonium chloride (18.0 g, 0.34 mol) were dissolved in 100 mL of water and 200 mL of alcohol. The mixture was heated to the reflux temperature (about 75 °C) and reacted for 6 h. After the reaction, the mixture was poured into plenty of water and the precipitate was collected by filtration. The product was dried in vacuum oven at 70 °C for 24 h.

Synthesis of *N,N*-di(hydroxyethyl)aniline biscinnamate. *N,N*-di(hydroxyethyl)aniline (18.1 g, 0.1 mol)

and triethylamine (42 mL) were dissolved in DCM (100 mL) and the mixture was stirred in an ice-water bath. Cinnamoyl chloride (40 g, 0.24 mol) was added dropwise into the mixture. The mixture was reacted in an ice-water bath for 24 h. After the reaction, the mixture was washed with saturated salt water and then the organic solvent phase was dried with anhydrous MgSO_4 . Yellow thick liquid was obtained by column chromatography (eluent: DCM/EA=10/1).



Scheme S1. Synthesis route of IAC-4.

Synthesis of IAC-4. IAC-4 was synthesized by azo-coupling reaction between isosorbide *bis*(4-aminobenzoate) and *N,N*-*di*(hydroxyethyl)aniline *biscinnamate*. *N,N*-*di*(hydroxyethyl)aniline *biscinnamate* (2.05 g, 0.0047 mol) was dissolved in DMF (100 mL) and stirred in an ice-water bath. Isosorbide *bis*(4-aminobenzoate) (0.59 g, 0.0016 mol) was mixed with glacial acetic acid (9 mL) and sulfuric acid (0.9 mL) in an ice-water bath. The mixture was stirred at 0 °C for 2 h until no solid existed. The diazonium salt was prepared by adding an aqueous solution of NaNO_2 (0.31 g, 0.0045 mol in 0.9 mL water) into the mixture of isosorbide *bis*(4-aminobenzoate). Homogeneous solution obtained by stirring with ice-water bath cooling was added dropwise into the DMF solution of *N,N*-*di*(hydroxyethyl)aniline *biscinnamate*. The solution was reacted at 0 °C for 12 h. After the reaction, the mixture was added into plenty of water, and the precipitate was collected by filtration. Red solid was obtained through column chromatography (eluent: DCM/EA=10/1).

2. Structure characterization of BP-AZ-CA and IAC-4

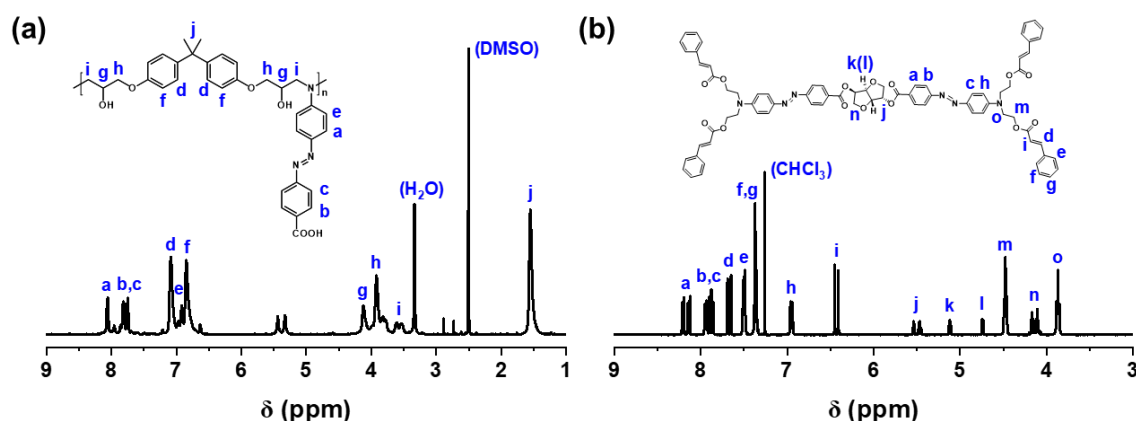


Fig. S1 ^1H NMR spectra of azo-chromophore-containing polymer and molecular glass, (a) BP-AZ-CA and (b) IAC-4 with the resonance signal assignment.

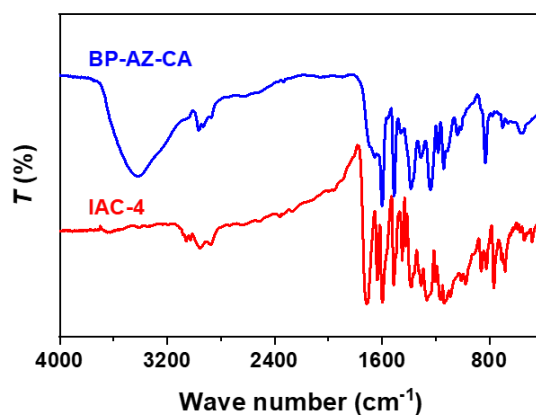


Fig. S2 FT-IR spectra of BP-AZ-CA and IAC-4.

3. Physical and chemical properties of BP-AZ-CA and IAC-4

Table S1 Some physical and chemical properties of BP-AZ-CA and IAC-4.

	Molecular weight	λ_{max} (nm)	ϵ at 488 nm ($\text{L}\cdot\text{g}^{-1}\cdot\text{cm}^{-1}$)	T_g ($^{\circ}\text{C}$)	T_d ($^{\circ}\text{C}$)	Nanoindentation modulus (GPa)	DMT modulus by AFM (GPa)
BP-AZ-CA	17000 (M_n) $M_w/M_n=1.82$	440 (in DMF) 433 (thin film)	22.0 (in DMF)	155	250	5.6 ± 0.1	6.1 ± 0.4
IAC-4	1289.4	443 (in DMF) 434 (thin film)	29.6 (in DMF)	63	335	4.0 ± 0.2	4.2 ± 0.3

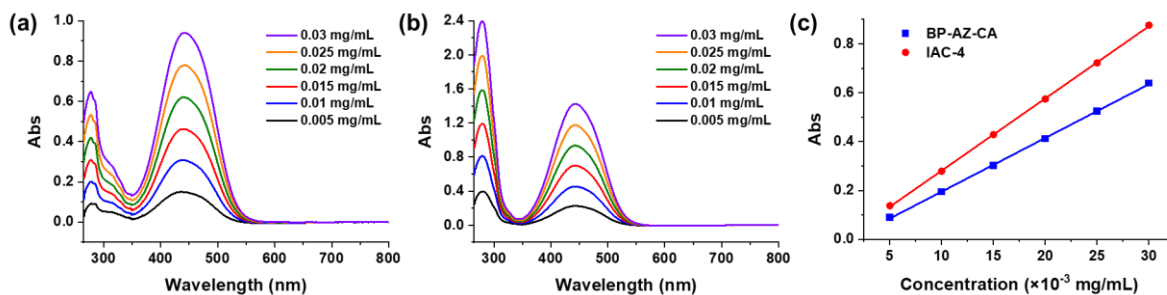


Fig. S3 UV-vis spectra of (a) BP-AZ-CA and (b) IAC-4 in DMF solutions with different concentrations; (c) relationship between the absorbances and the concentrations of BP-AZ-CA and IAC-4 in DMF solutions, obtained from the UV-vis spectra at $\lambda = 488$ nm.

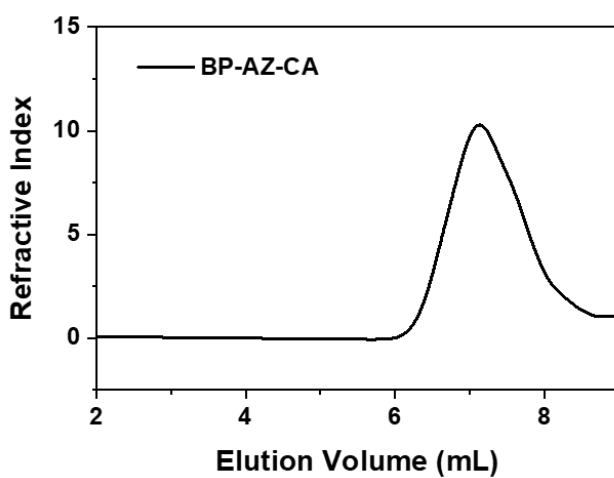


Fig. S4 GPC curve of the azo polymer BP-AZ-CA with THF as the eluent, $M_w = 31000 \text{ g}\cdot\text{mol}^{-1}$, $M_n = 17000 \text{ g}\cdot\text{mol}^{-1}$, $M_w/M_n = 1.82$.

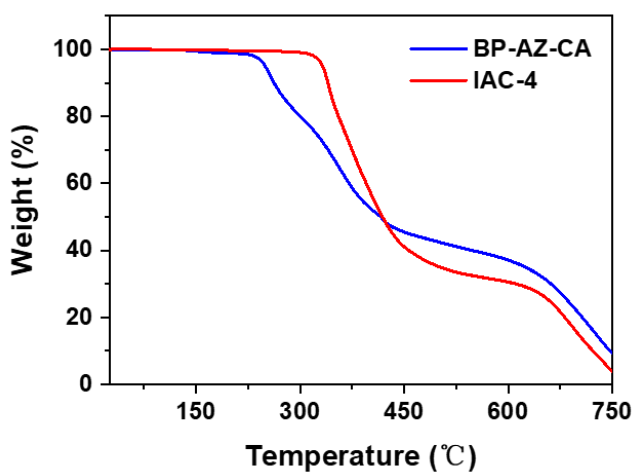


Fig. S5 TGA curves of BP-AZ-CA and IAC-4.

4. Morphological characterization of films and SRGs

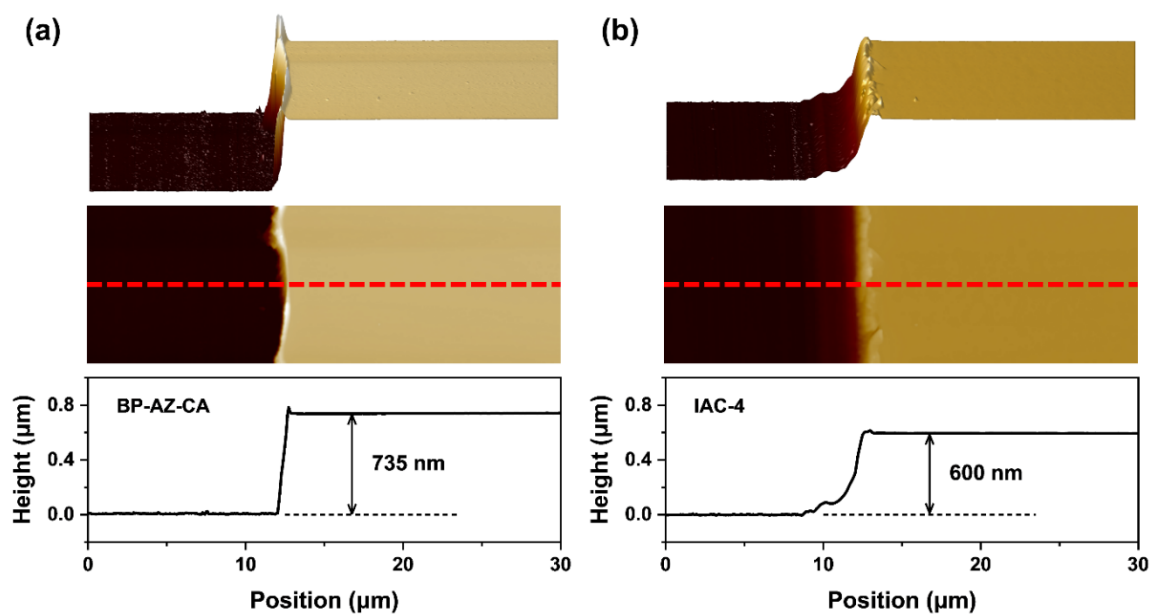


Fig. S6 Topographical AFM images (3D view and 2D view) of (a) BP-AZ-CA and (b) IAC-4 films with the scratch. From the height section view, the thicknesses of BP-AZ-CA and IAC-4 films are around 735 nm and 600 nm, respectively.

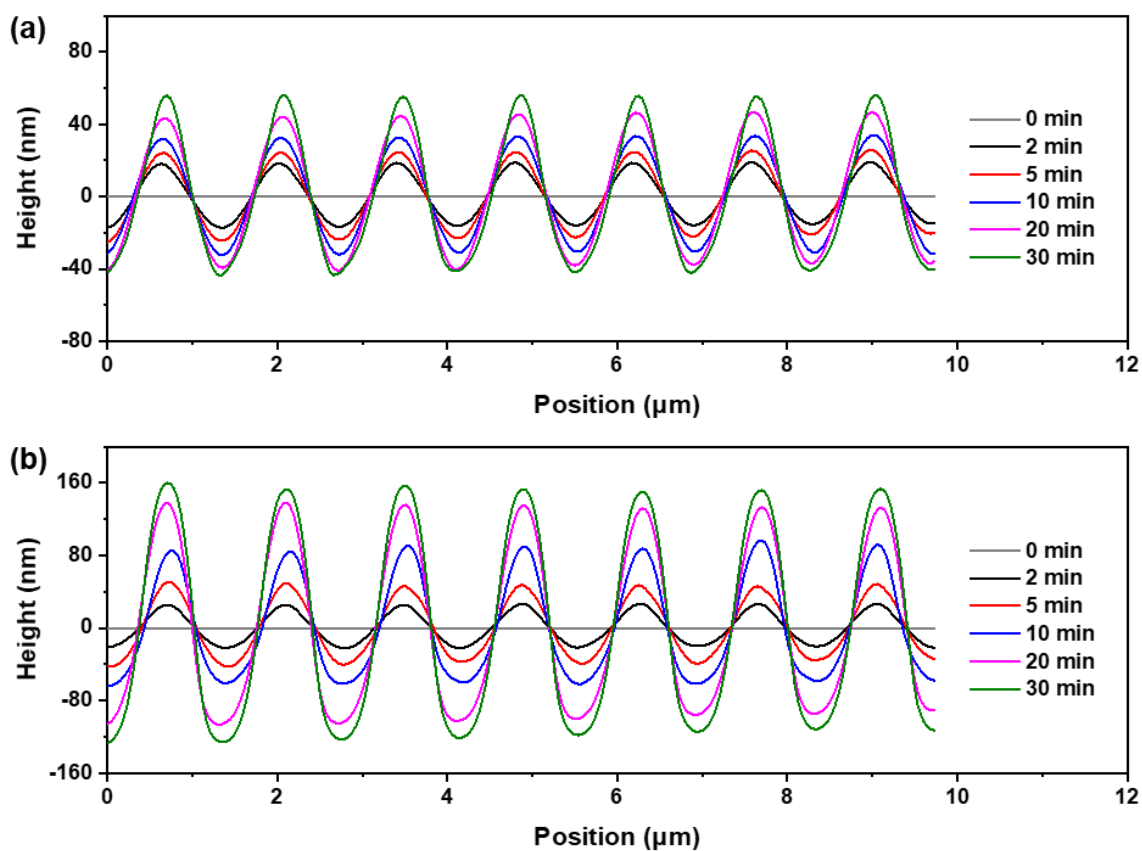


Fig. S7 Variations of height sections of surface relief gratings ($p = 1400$ nm) formed on (a) BP-AZ-CA and (b) IAC-4 films with the irradiation time.

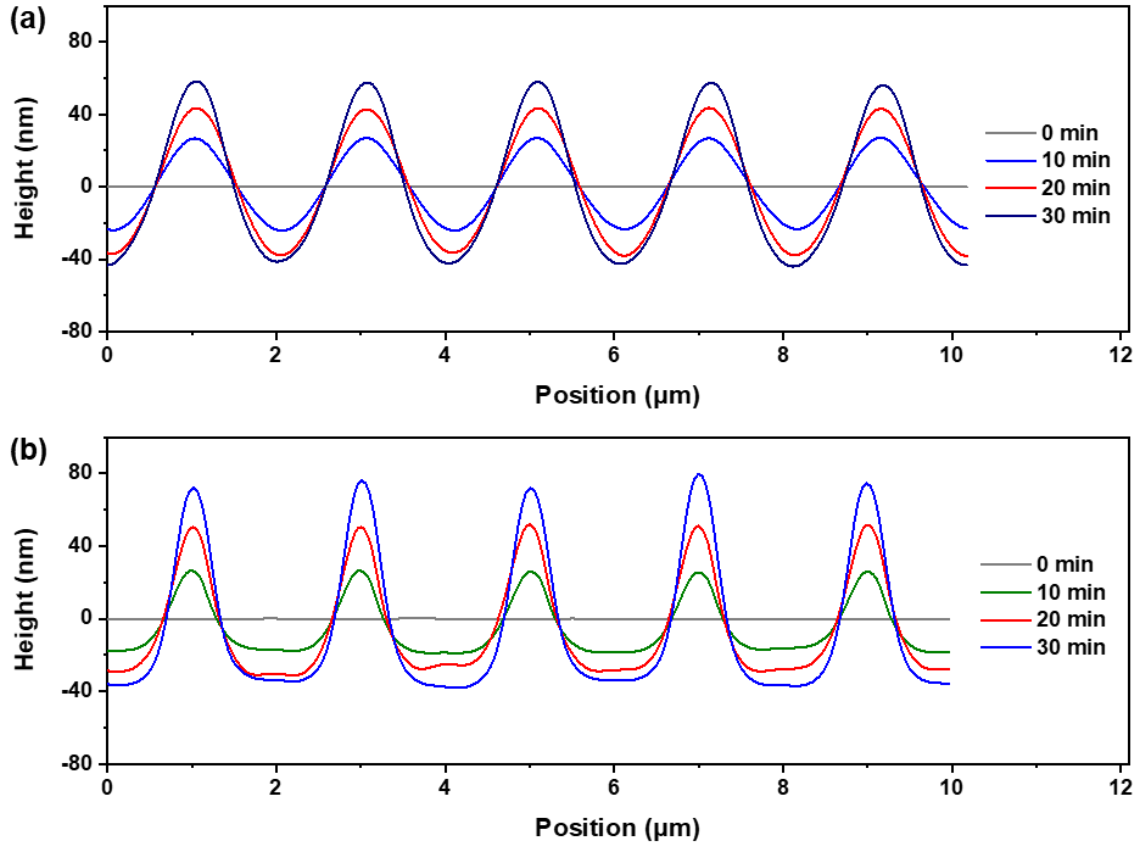


Fig. S8 Variations of height sections of surface relief gratings ($p = 2000$ nm) formed on (a) BP-AZ-CA and (b) IAC-4 films with the irradiation time.

5. Calculation of the thermal effect upon laser irradiation

The thermal effect of BP-AZ-CA and IAC-4 films upon laser irradiation was calculated using the model shown in Fig. S9. The spin-coated film on the glass substrate is illuminated by the interference pattern formed by two coherent laser beams, both of which show the intensity (I_0) of 100 mW/cm^2 . The illumination region has a semicircle shape (painted by red color in Fig. S9), as half of the collimated beam (a circular beam spot with the radius of r) is directly incident on the film and the other half of the beam is reflected onto the film from the Lloyd mirror. Considering the thickness of film (from 600 nm to 800 nm) is much smaller than the thickness of glass substrate ($z_g = 1.1 \text{ mm}$), the temperature of film can be regarded as that of the substrate beneath it. Consequently, the thin film layer is not considered in the model, and the temperature distribution of glass substrate is calculated to evaluate the photo-thermal effect of the spin-coated film upon laser irradiation.

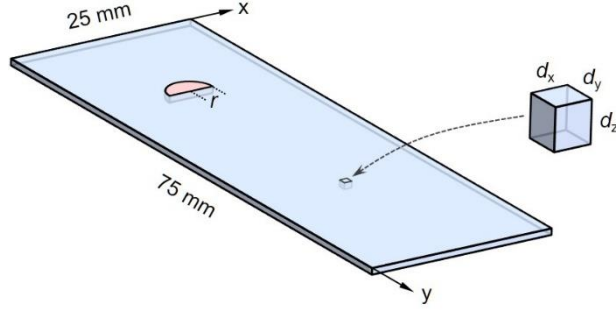


Fig. S9 Schematic illustration of the thermal calculation model.

The glass substrate shown in Fig. S9, with the dimension of $l_g \times w_g \times z_g = 75 \text{ mm} \times 25 \text{ mm} \times 1.1 \text{ mm}$, is divided into the mesh with the size of $dx \times dy \times dz = 1 \text{ mm} \times 1 \text{ mm} \times 1.1 \text{ mm}$. The temperature of each mesh at heat balance is calculated by the energy conservation law,

$$-k \left(\frac{\partial^2 T}{\partial x^2} + \frac{\partial^2 T}{\partial y^2} \right) + \frac{h(T - T_{\text{air}})S}{V} = q_a \quad (\text{S1})$$

The first term in the left hand side of Equation (S1) represents the heat conduction to the adjacent mesh, which follows the Fourier's Law.^{S3} The heat conductivity (k) of glass is $1.4 \text{ W} \cdot \text{K}^{-1} \cdot \text{m}^{-1}$. For the mesh with finite size, the second order derivative is calculated by the central difference form,

$$\frac{\partial^2 T}{\partial x^2}(x, y) = \frac{T_{x+dx, y} + T_{x-dx, y} - 2T_{x, y}}{dx^2} \quad (\text{S2})$$

$$\frac{\partial^2 T}{\partial y^2}(x, y) = \frac{T_{x, y+dy} + T_{x, y-dy} - 2T_{x, y}}{dy^2} \quad (\text{S3})$$

where $T_{x, y}$ is the temperature of mesh at the coordinate of (x, y) .

The second term in the left hand side of Equation (S1) represents the heat convection on the surface of substrate, which is known as the Newton's Law of Cooling.^{S3} h is the heat transfer coefficient of natural convection and estimated to have a value of 20 W/K/m^2 . T_{air} is the temperature of the ambient air (299.15 K , $26 \text{ }^\circ\text{C}$). S is the area corresponding to the convective heat flux (the surface area of mesh in contact with air), which is $2dxdy$ for the inner mesh, $dxdy+dxdz$ (or $dxdy+dydz$) for the edge mesh and $dxdy/2+dxdz/2+dydz/2$ for the corner mesh. V is the volume of each mesh, which is $dxdydz$ for the inner mesh, $dxdydz/2$ for the edge mesh and $dxdydz/4$ for the corner mesh, respectively.

The heat source (q_a) is generated by the light absorption of spin-coated film (unit: W/m³), which is regarded to be distributed in the whole mesh in the illuminated region. This simplification is valid as the glass substrate is thin ($z_g = 1.1$ mm) and the heat transfer in z-direction is very efficient. Consequently, q_a in the illumination region can be expressed by,

$$q_a = \frac{2aI_0}{z_g} \quad (S4)$$

where a is the coefficient of absorption efficiency of the spin-coated film, which is less than 1 as the incident light is partially reflected on the film surface and transmitted through the film. By respectively evaluating these two factors by Fresnel equation and Lambert-Beer's Law,^{S4} a is determined to be 0.88, which is applicable for both BP-AZ-CA and IAC-4 as they show similar light absorption ability and similar film thickness. In the un-illuminated region, q_a is zero.

Finally, the temperature distribution of the model is calculated by combining Equation (S1-S4) and solving a set of linear equations. The average temperature in the illumination region for r ranging from 3 mm to 9 mm is listed in Table S2, which agrees well with the measured values. For $r = 3$ mm, which was used in experiments to inscribe SRG, the maximum temperature of the spin-coated azo film upon two-beam irradiation is only about 30.3 °C, obviously lower than the glass transition temperatures of BP-AZ-CA and IAC-4. Therefore, the two materials are still in the glassy state after the light irradiation.

Table S2 Temperatures of the films when exposed to the interference light of two coherent laser beams with different spot radii.

Light Spot Radius	3 mm	5 mm	7 mm	9 mm
BP-AZ-CA film (Measured)	29 °C	31 °C	35 °C	37 °C
IAC-4 film (Measured)	29 °C	32 °C	35 °C	38 °C
Simulated	29.6 °C	33.0 °C	36.5 °C	39.9 °C

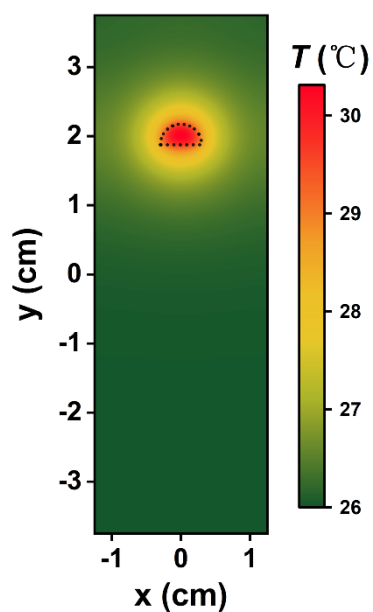


Fig. S10 Simulated temperature distribution of the spin-coated film on the glass substrate upon exposure to the interference field of two coherent laser beams with the light spot radius of 3 mm.

6. Nanomechanical properties of azo films

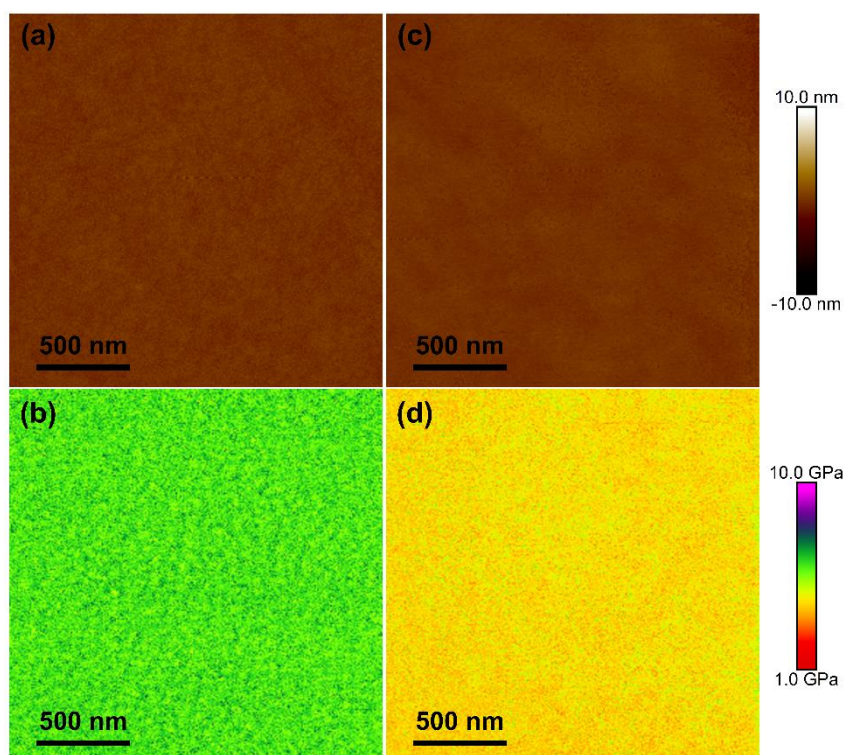


Fig. S11 Height map (a) and corresponding DMT modulus map (b) of BP-AZ-CA film; height map (c) and corresponding DMT modulus map (d) of IAC-4 film.

7. Characterization of the AFM probe

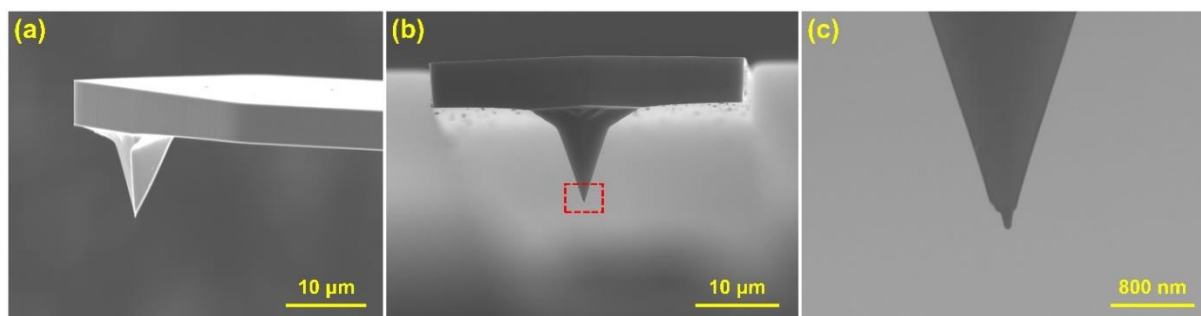


Fig. S12 SEM images of the AFM probe (RTESPA-525) used in the experiments: (a) side view; (b) front view; (c) enlarged view of the dashed rectangle area shown in (b).

8. Preparation of submicron arrays on IAC-4 films

Periodic submicron hexagonal pillar and hole arrays of IAC-4 were prepared by hot embossing with its films according to literature.^{S5} Thin solid films of IAC-4 with a smooth surface were prepared by spin-coating of an IAC-4 solution in DMF (20% w/v). The PDMS molds with periodic holes and pillars on the surface used for the hot embossing were obtained from the commercial source (Gd nano Co., Ltd). For the hot embossing, the PDMS molds were placed and kept in seamless touch with the IAC-4 film surface. The molds and IAC-4 films were heated together on a hot stage to 110 °C. The molds were then pressed downward with a gentle pressure for 30 min and the temperature was gradually lowered to 30 °C, while keeping the molds in conformal touch with the IAC-4 films. After that, the PDMS molds were peeled off at 30 °C to obtain the submicron pillar and hole arrays.

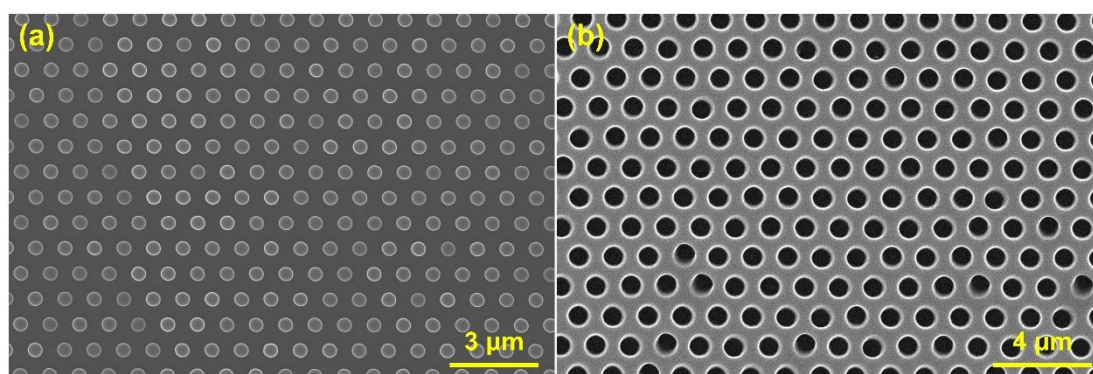


Fig. S13 SEM images of the periodic submicron hexagonal (a) pillar array and (b) hole array prepared on IAC-4 films through microcontact hot embossing with elastomeric PDMS molds.

References

- S1 Y. N. He, X. G. Wang and Q. X. Zhou, *Polymer*, 2002, **43**, 7325–7333.
- S2 M. C. Guo, Z. D. Xu and X. G. Wang, *Langmuir*, 2008, **24**, 2740–2745.
- S3 F. P. Incropera, D. P. DeWitt, T. L. Bergman and A. S. Lavine, *Fundamentals of Heat and Mass Transfer*, Wiley, New York, 7th ed., 2011.
- S4 A. Lipson, S. G. Lipson and H. Lipson, *Optical Physics*, Cambridge University Press, Cambridge, 4th ed., 2010.
- S5 C. E. Hsu, Z. D. Xu and X. G. Wang, *Adv. Funct. Mater.*, 2018, **28**, 1802506.